Protection and Control of Modern Power Systems

ORIGINAL RESEARCH Open Access

A robust composite wide area control of a DFIG wind energy system for damping inter-area oscillations

Ayyarao S. L. V. Tummala

Abstract

This paper presents a novel composite wide area control of a DFIG wind energy system which combines the Robust Exact Differentiator (RED) and Discontinuous Integral (DI) control to damp out inter-area oscillations. RED generates the real-time differentiation of a relative speed signal in a noisy environment while DI control, an extension to a twisting algorithm and PID control, develops a continuous control signal and hence reduces chattering. The proposed control is robust to disturbances and can enhance the overall stability of the system. The proposed composite sliding mode control is evaluated using a modified benchmark two-area power system model with wind energy integration. Simulation results under various operating scenarios show the efficacy of the proposed approach.

Keywords: DFIG, Wide area control, Wind energy system, Sliding mode control

1 Introduction

Increases in energy demand and environmental awareness, government clean energy policies, increased inflow of funds and reduced cost have resulted in huge renewable energy development and generation [1]. Among the different renewable power generation methods, wind energy dominates because of its mature technology and the abundant wind resources in many nations. According to Navigant Research, 51.3 GW capacity of wind energy was installed in 2018, reflecting the interests among producers and governments for cheap and clean renewable energy generation. Doubly fed induction generators (DFIGs) are one of the main wind-energy conversion systems (WECS) [2, 3]. They are extensively used owing to features like reduced converter rating, two-degree freedom in controlling active and reactive power and high conversion efficiency. A DFIG wind energy system with conventional vector control regulates active and reactive power independently, while its active power reference is computed based on the maximum power point tracking, which in turn depends on the wind speed [4, 5]. As the performance of a DFIG system largely depends on the control, early research was mainly focused on the optimal DFIG control by tuning the controller parameters [6, 7]. Emphasis was then gradually moved towards application of nonlinear control techniques [8–11].

Transmission interconnections are necessary for reliable and efficient operation of the power system. Integration of renewable energy with the grid reduces the inertia of the system and may adversely affect system stability [12]. Conventional power system stabilizers are deployed at generating stations with synchronous generators to suppress power oscillations. However, the performance of these stabilizers is limited to local modes, while FACTS controllers like SVC, STATCOM, and UPFC have been used to mitigate inter-area oscillations [13–15]. The installation of PMUs at various nodes in the power system enables continuous monitoring of inter-area oscillations. The use of a PSS-based supplementary damping controller in a DFIG system to reduce inter-area oscillations is implemented in [16]. However, preliminary research was focused on developing supplementary control using active

Correspondence: ayyarao.tslv@gmrit.edu.in; ayyarao.tummala@gmail.com
Department of EEE, GMR Institute of Technology, Rajam 532127, India

power, whereas it has been observed that reactive power regulation can be more effective [17]. Thus, suppression of inter-area oscillations could be further enhanced by regulating both active power and reactive power output of the DFIG system [18]. Proportional-resonant controller-based power oscillation damping is proposed in [19], while most of the research on damping of inter-area oscillations is based on a lead-lag compensator [20–22]. However, the performance of the controller cannot be assured for large disturbances in the system as the design is based on a linearized model of the power system around an operating point.

Nonlinear control methods like input-output linearization, adaptive dynamic programming etc. have been developed [23, 24]. As power system networks are highly distributed and can exposed to many types of disturbance, there is a need to develop robust controllers. Additional damping control based on disturbance rejection is proposed in [25], and a wide-area control design based on line potential energy and an extended state observer is proposed in [26]. However, such controllers encounter a key challenge in guaranteeing finite time output tracking. Sliding mode control is a robust control mechanism that can ensure finite time output tracking, so a second order sliding mode based on twisting law is proposed in [27, 28]. However, although it is highly robust, the output of the differentiator is sensitive to measurement noise.

The objective of this paper is to design a robust composite wide area controller (WAC) for a DFIG wind energy system, combined with RED and DI controls. DI control is a recently proposed novel control based on the combination of the super twisting algorithm (STA) and PID control. To compensate for the non-vanishing disturbances, a discontinuous integral term is added to the STA control output and a two-stage differentiator is developed to obtain the real-time differentiation of the relative speed signal. This is robust to measurement noise and uncertainties [29, 30]. Features viz. finite-time convergence, robustness to disturbance and reduced chattering are achieved by applying DI control [31, 32]. A supplementary WAC signal is thus generated to regulate the reactive power of a DFIG system through its RSC.

The main contributions of the paper are as follows:

i. A composite wide area control combined with a robust differentiator with discontinuous integral control is proposed to suppress inter-area oscillations using a DFIG based wind energy system.
ii. The use of RED is to obtain a real-time differentiation of the relative speed immune to noise in the PMU measurements. A DI controller generates a continuous control signal and thus reduces the chattering.
iii. The proposed strategy is simple to implement and is robust to disturbances.

The rest of the paper is organized as follows. Section 2 discusses the dynamics of the two-area power system model with a DFIG in one area, while Section 3 describes the design of the proposed composite wide area control. Section 4 analyzes the simulation results with the proposed controller and concluding remarks are given in Section 5.

2 System configuration and dynamic model of a DFIG system

2.1 Modified two-area power system with wind energy integration

The system under study is a modified two-area benchmark model integrated with a DFIG-based wind energy system as shown in Fig. 1. Area-1 consists of a hydraulic generator while area-2 has a synchronous generator. These two areas are connected by a transmission line while a DFIG-based wind power plant is connected to Area-1. A resistive load is connected to Area-2 and power flows from Area-1 to Area-2.

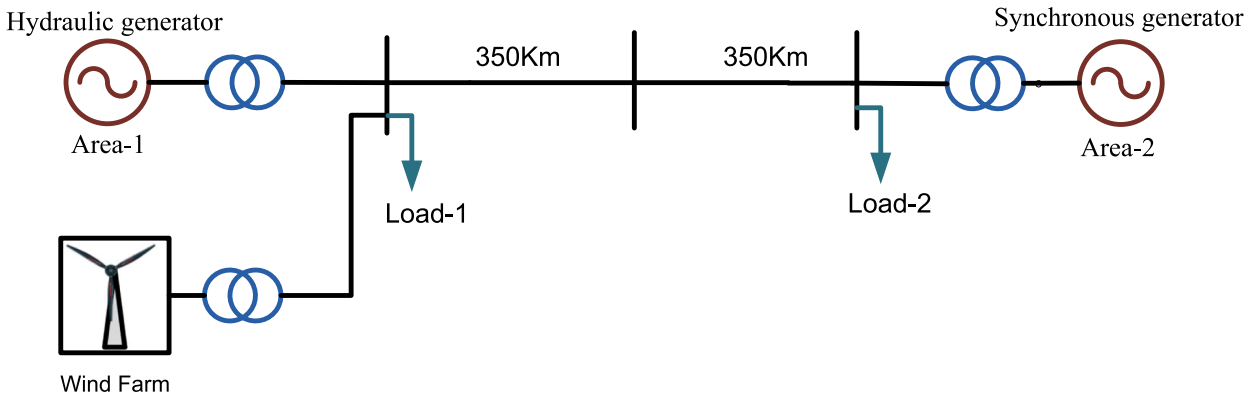

Fig. 1 Modified two-area power system model with wind energy integration

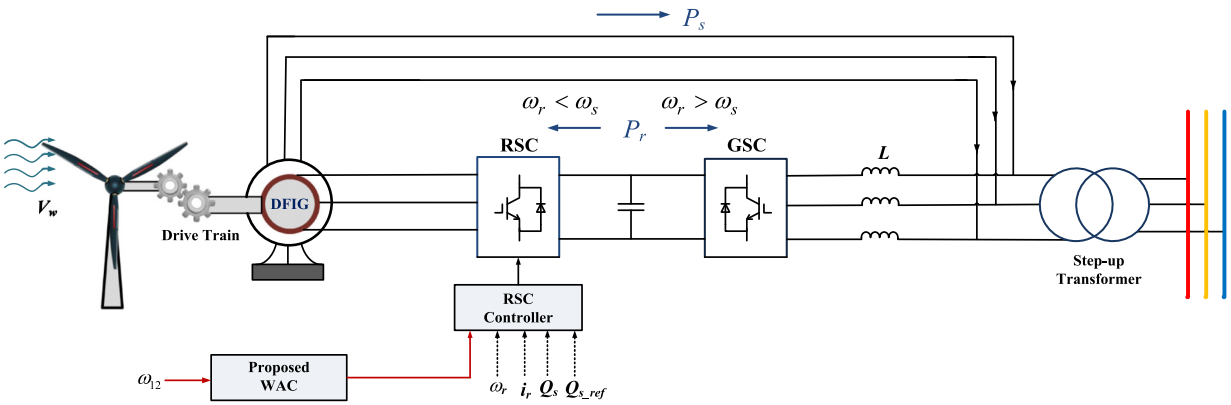

Fig. 2 DFIG wind energy system with WAC

The dynamics of the two-area power system model with wind energy integration [27] are given as:

$$\dot{\delta}_{12} = \omega_{12} \quad (1)$$

$$\dot{\omega}_{12} = \frac{1}{H_1}(P_1 - P_{L1}) - \frac{1}{H_2}(P_2 - P_{L2}) + \left(\frac{1}{H_1} + \frac{1}{H_2}\right)\frac{\sin\delta}{\cos\delta}\left(\frac{V_2^2}{X} - \Delta Q_w - Q_w - Q_{s0}\right) \quad (2)$$

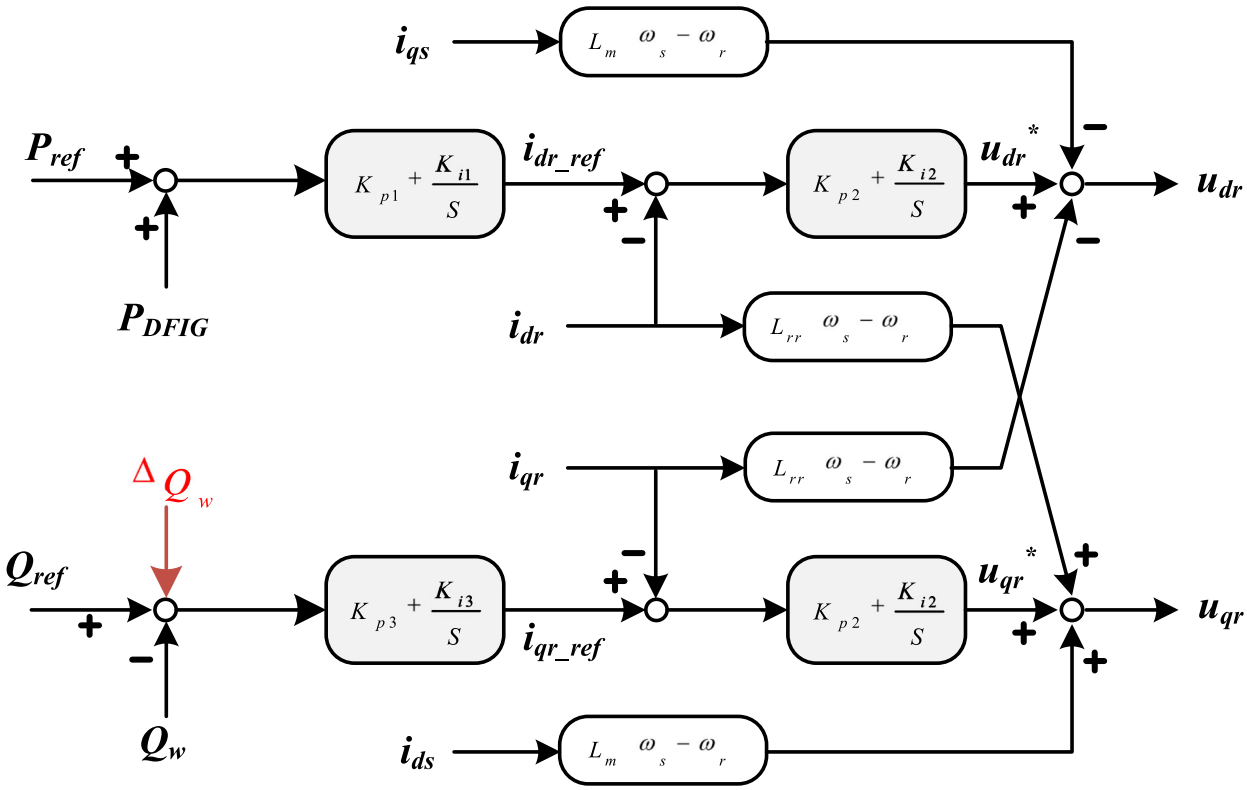

Fig. 3 Block diagram of the RSC controller

$$\Delta\dot{Q}_w = \frac{u - \Delta Q_w}{T} \quad (3)$$

2.2 Dynamic model of DFIG

A DFIG wind energy system consists of a wind turbine coupled to the DFIG shaft. The output of the DFIG system is regulated by a back-to-back converter, in which the GSC regulates the DC link voltage while the RSC regulates both the active and reactive power output. To suppress inter-area oscillations, a supplementary control signal is generated from the proposed WAC unit to regulate the reactive power output of the DFIG system as illustrated in Fig. 2. As the main objective is to suppress the oscillations, this section focuses on the dynamic model of the DFIG machine and RSC control.

The dynamic model of a DFIG generator is represented as:

$$\frac{dE_d^{'}}{dt} = s_r\omega_s E_q^{'} - \omega_s \frac{L_m}{L_{rr}} u_{qr} - \frac{1}{T_0^{'}}\left[E_d^{'} + \left(X_s - X_s^{'}\right) i_{qs}\right] \quad (4)$$

$$\frac{dE_q^{'}}{dt} = -s_r\omega_s E_d^{'} + \omega_s \frac{L_m}{L_{rr}} u_{dr} - \frac{1}{T_0^{'}}\left[E_q^{'} - \left(X_s - X_s^{'}\right) i_{ds}\right] \quad (5)$$

$$\frac{di_{ds}}{dt} = \frac{\omega_s}{X_s^{'}}\left\{\begin{array}{l} u_{ds} - \left[R_s + \frac{1}{\omega_s T_0^{'}}\left(X_s - X_s^{'}\right)\right] i_{ds} - \\ (1 - s_r) E_d^{'} - \frac{L_m}{L_{rr}} u_{dr} \end{array}\right\} + \frac{1}{X_s^{'} T_0^{'}} E_q^{'} + \omega_s i_{qs} \quad (6)$$

$$\frac{di_{qs}}{dt} = \frac{\omega_s}{X_s^{'}}\left\{\begin{array}{l} u_{qs} - \left[R_s + \frac{1}{\omega_s T_0^{'}}\left(X_s - X_s^{'}\right)\right] i_{qs} - \\ (1 - s_r) E_q^{'} - \frac{L_m}{L_{rr}} u_{qr} \end{array}\right\} - \frac{1}{X_s^{'} T_0^{'}} E_d^{'} - \omega_s i_{ds} \quad (7)$$

The outer and inner loop controls are based on PI controllers as illustrated in Fig. 3. The active and reactive power deviations are defined as:

$$e_p = P_{ref} - P_g \quad (8)$$

$$e_w = Q_{ref} - Q_w - \Delta Q_w \quad (9)$$

These errors are fed to the PI controllers to generate the reference d-axis and q-axis current as:

$$i_{dr\_ref} = K_{p1} e_p + K_{i1} \int e_p dt \quad (10)$$

$$i_{qr\_ref} = K_{p3} e_Q + K_{i3} \int e_w dt \quad (11)$$

The current references are compared with actual current to generate current errors as:

$$e_d = i_{dr} - i_{dr\_ref} \quad (12)$$

$$e_q = i_{qr} - i_{qr\_ref} \quad (13)$$

The current errors are then fed to the PI controllers to generate the control voltages as:

$$u^*_{dr} = K_{p2} e_d + K_{i1} \int e_d dt \quad (14)$$

$$u^*_{qr} = K_{p2} e_q + K_{i2} \int e_q dt \quad (15)$$

3 Design of composite wide area damping control (WAC)

The objective is to damp out rotor speed oscillation in finite time with a robust WAC, i.e. $\lim_{t \to t_f} \omega_{12} \to 0$. To achieve this, a combination of RED and DI controls is proposed.

3.1 DI control

The design of the DI control law is presented in this section. Considering the sliding variable as

$$\sigma = \omega_{12} \quad (16)$$

the second derivative of σ with respect to time is:

$$\sigma = -\left(\frac{1}{H_1} + \frac{1}{H_2}\right)\left(\frac{V_2^2}{X} - \Delta Q_w - Q_w - Q_{s0}\right)\frac{\omega_{12}}{\cos^2} - \left(\frac{1}{H_1} + \frac{1}{H_2}\right)\frac{\Delta Q_w \sin\delta}{T\cos\delta} + \left(\frac{1}{H_1} + \frac{1}{H_2}\right)\frac{\sin\delta}{T\cos\delta} u \quad (17)$$

Equation (17) can be represented as:

$$\ddot{\sigma} = f(\omega_{12}, \delta, t) + g(\delta, t) u \quad (18)$$

where

$$f = -\left(\frac{1}{H_1} + \frac{1}{H_2}\right)\left(\left(\frac{V_2^2}{X} - \Delta Q_w - Q_w - Q_{s0}\right)\frac{\omega_{12}}{\cos^2} + \frac{\Delta Q_w \sin\delta}{T\cos\delta}\right)$$

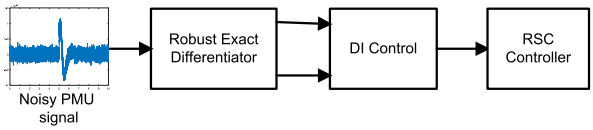

Fig. 4 Proposed Composite Controller

$$g = \left(\frac{1}{H_1} + \frac{1}{H_2}\right)\frac{\sin\delta}{T\cos\delta}$$

Equation (17) can also be rewritten as:

$$\ddot{\sigma} = f(\omega_{12}, \delta, t) + u_c \tag{19}$$

where

$$u_c = g(\delta, t)u \tag{20}$$

Though sliding mode control is robust when regulating output in the presence of disturbances, it suffers from control chattering. On the other hand, PID is effective in driving the output to the horizon but only in the presence of constant disturbances. In order to drive the states σ and $\dot{\sigma}$ in finite time in the presence of time-varying disturbances, a robust DI control is proposed which is a combination of a twisting algorithm and PID control [31]. An integral term is added to the regular high order sliding mode control law to compensate for the time varying perturbations which cannot be fully compensated for by feedback discontinuous control.

The control law required to stabilize the system under persistent disturbances is given by:

$$u_c = -\lambda_1|\sigma|^{\frac{1}{3}}\,\mathrm{sgn}(\sigma) - \lambda_2\left|\dot{\sigma}\right|\,\mathrm{sgn}\left(\dot{\sigma}\right) - \lambda_3\int \mathrm{sgn}\left(\sigma + \lambda_4\dot{\sigma}^{\frac{3}{2}}\right)d\tau \tag{21}$$

From (20) and (21), there is:

$$u = \frac{1}{g^{-1}(\delta, t)}\left(-\lambda_1|\sigma|^{\frac{1}{3}}\,\mathrm{sgn}(\sigma) - \lambda_2\left|\dot{\sigma}\right|\,\mathrm{sgn}\left(\dot{\sigma}\right) - \lambda_3\int \mathrm{sgn}\left(\sigma + \lambda_4\dot{\sigma}^{\frac{3}{2}}\right)d\tau\right) \tag{22}$$

The main features of the proposed robust control law are:

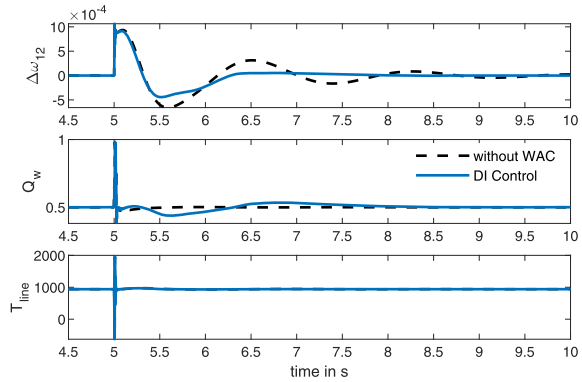

Fig. 5 a Relative rotor speed deviations; **b** Reactive power; **c** Tie-line power deviations for a three-phase fault with a fault resistance of 1 Ω

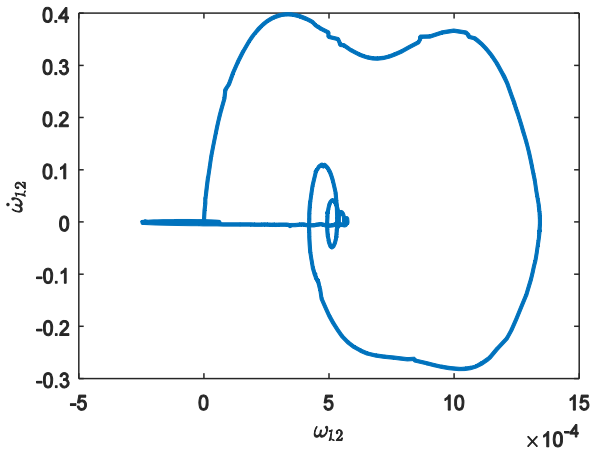

Fig. 6 2D plot of σ and $\dot{\sigma}$

i. It stabilizes the origin in finite time. In addition, adding a discontinuous integral term stabilizes the system even under non-vanishing disturbances.
ii. The continuous control signal avoids control chattering.
iii. The integral term can be viewed as disturbance estimation.
iv. Implementation of the discontinuous integral control requires the derivative of ω_{12}.

3.2 Robust exact differentiator

An ordinary differentiator amplifies measurement noise, and thus noisy PMU measurements degrade the performance of the controller with ordinary differentiator. In addition, initial error and large transients during convergence of the differentiator will degrade the controller performance. Therefore, there is a need for a robust exact differentiator. Considering its advantages such as finite time convergence, robustness to external disturbances and insensitivity to measurement noise,

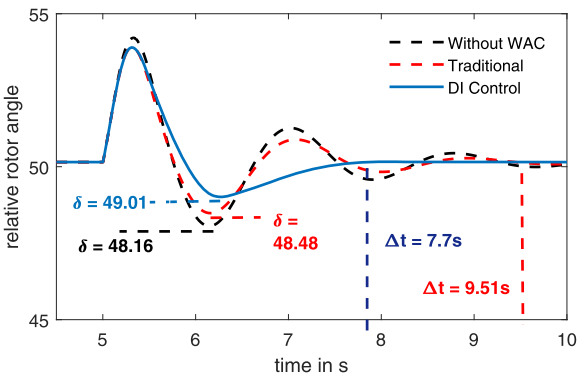

Fig. 7 Relative rotor angle deviations for a three-phase fault with a fault resistance of 0.001 Ω

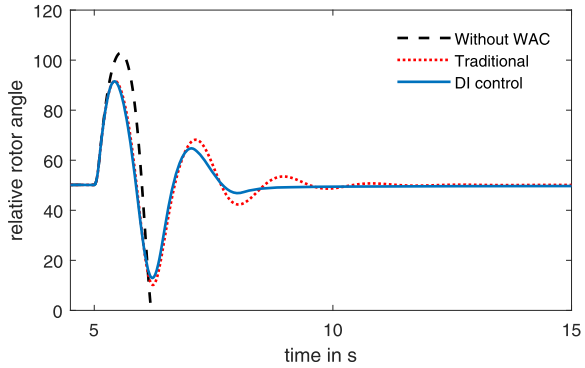

Fig. 8 Relative rotor angle deviations in the worst fault scenario

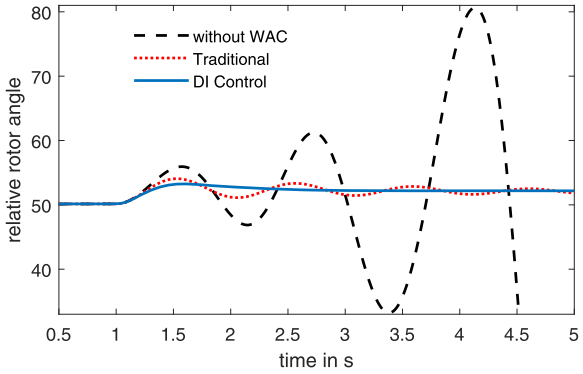

Fig. 10 Relative rotor angle for load disturbance

RED is used here to obtain the differentiation of the relative speed signal.

The output of the system in the presence of noise can be written as:

$$y = \omega_{12} + \nu \tag{23}$$

A second order RED is employed to estimate the signal $\dot{\sigma}$. Given that z_1 and z_2 are the respective estimates of σ and $\dot{\sigma}$, and d is the cumulative disturbance of the system estimated with a pseudo-state z_3, the dynamics of RED are:

$$\dot{z_1} = -l^{\frac{1}{3}}\lambda_1|z_1 - y|^{\frac{2}{3}}\,\mathrm{sgn}(z_1 - y) + z_2 \quad (24)$$

$$\dot{z_1} = -l^{\frac{1}{3}}\lambda_1|z_1 - y|^{\frac{2}{3}}\,\mathrm{sgn}(z_1 - y) + z_2 \quad (25)$$

$$\dot{z_3} = -l\lambda_3\,\mathrm{sgn}(z_1 - y) \quad (26)$$

3.3 Composite WAC

The principle of the proposed composite controller is illustrated in Fig. 4. It is a combination of DI control and RED. With the observed states the new control input is:

$$u_c = -\lambda_1|z_1|^{\frac{1}{3}}\,\mathrm{sgn}(z_1) - \lambda_2|z_2|\,\mathrm{sgn}\left(\dot{\sigma}\right) - \lambda_3\int \mathrm{sgn}\left(z_1 + \lambda_4 z_2^{\frac{3}{2}}\right)d\tau \tag{27}$$

Defining the estimation errors as $e_1 = x_1 - z_1$, $e_2 = x_2 - z_2$, and $e_3 = x_3 - d$, the dynamics of the estimation errors can be written as:

$$\dot{e_1} = -l^{\frac{1}{3}}\lambda_1|e_1|^{\frac{2}{3}}\,\mathrm{sgn}(e_1) + e_2 \quad (28)$$

$$\dot{e_2} = -l^{\frac{2}{3}}\lambda_2|e_1|^{\frac{1}{3}}\,\mathrm{sgn}(e_1) + e_3 \quad (29)$$

$$\dot{e_3} = -l\lambda_3\,\mathrm{sgn}(e_1) - \dot{d} \quad (30)$$

From the above analysis, the following can be noted:

i. For $|\dot{d}| \le \Delta$, the estimation errors under closed loop operation converge to the origin in finite time.
ii. Control input compensates for the disturbance affecting system performance.
iii. The differentiator and controller can be designed independently.

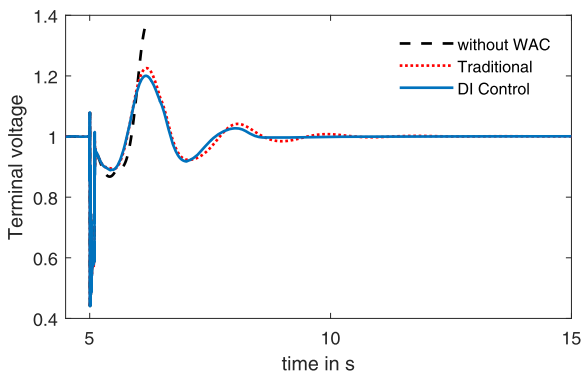

Fig. 9 Terminal voltage in the worst fault scenario

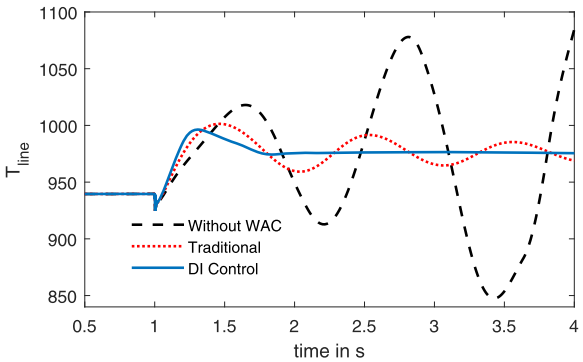

Fig. 11 Tie-line power deviations for load disturbance

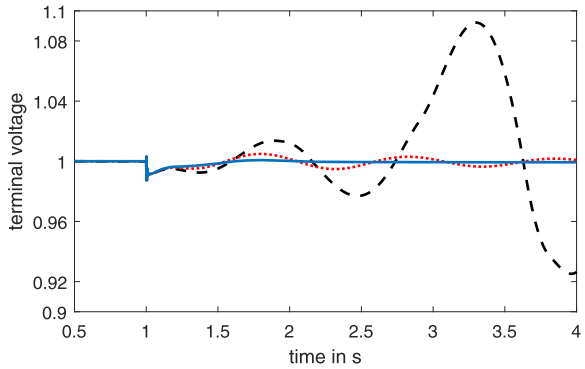

Fig. 12 Terminal voltage variations for load disturbance

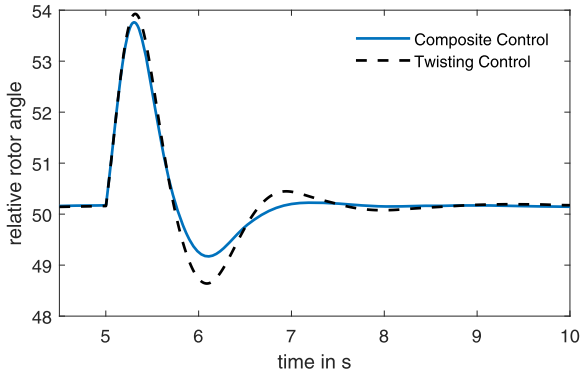

Fig. 14 Relative rotor speed in a noisy environment

4 Simulation results and discussion

The proposed composite control is simulated in MATLAB/Simulink. The benchmark system is obtained by modifying the two-area system demon model in MATLAB/ Simulink to include a DFIG wind energy system, while the parameters of the lumped DFIG and controller are given in Tables 1 and 2 respectively in the Appendix. The efficacy of the proposed approach is evaluated under different operating scenarios.

4.1 Noise-free measurements

In this ideal case, the measurements from PMU are assumed to be noise-free. The DI controller generates the required reactive power signal for suppression of the inter-area oscillations. The second state $\dot{\sigma}$ is obtained using the MATLAB differentiator block. In addition, a three-phase symmetrical fault is applied to the transmission line connecting the two areas. The fault is initiated at 5 s and cleared after 5 ms. This disturbance leads to rotor angle oscillation between the two areas as illustrated in Fig. 5 (a). In the absence of wide area control, the power oscillations are damped after 10s while with the proposed DI control, they are damped within 7.7 s. Reactive power outputs of the DFIG system with and without WAC can be observed from Fig. 5 (b). It can be observed that without WAC, the reactive power is not regulated while DI control regulates the reactive power. This demonstrates the superior performance of DI control in damping oscillations. The Tie-line power deviations with and without WAC are compared in Fig. 5 (c), while Fig. 6 depicts the convergence of σ and $\dot{\sigma}$ to the horizon.

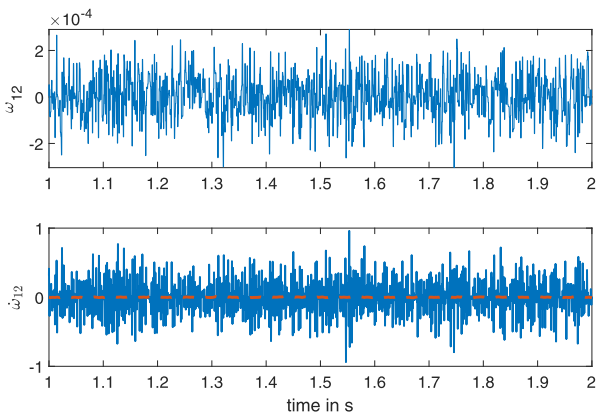

Fig. 13 Plots of **a** σ and **b** $\dot{\sigma}$ with and without RED. Red and blue colors represent with RED and ordinary differentiator respectively

Figure 7 illustrates the performance of DI control with rotor angle deviations for a three-phase fault with a fault resistance of 0.001 Ω. As can be seen, DI control damps out the rotor angle deviations faster with lower undershoot when compared to lead-lag compensator based traditional controller [17], whose details are given in Appendix. For further analysis, a worst fault scenario is considered where the system is unstable without WAC. The rotor angle deviations in Fig. 8 and terminal voltage in Fig. 9 show the efficacy of the proposed DI controller for the same worst fault scenario.

In the next case, it is assumed that the load is suddenly increased by 5% at 1 s, and the simulation results are shown in Figs. 10, 11 and 12. In order to evaluate the performance of the DI controller under the worst operating scenario, the synchronous generators are operated without local PSS. Without WAC, the load change leads to sustained rotor speed oscillations as seen in Fig. 10. However, the proposed DI controller effectively suppresses the relative rotor speed deviations and this also results in reduced tie-line power oscillations when compared to the traditional controller as illustrated in Fig. 11. The terminal voltage also oscillates in the absence of the WAC after the load disturbance while the proposed controller suppresses the voltage oscillations as shown in Fig. 12.

4.2 PMU measurements with noise

Table 1 DFIG Data

DFIG Data	
Nominal power	120 × 1.5 MW
Frequency	50 Hz
Stator Resistance R_s	0.00706 p.u
Stator Inductance L_s	0.171 p.u
Rotor Resistance R_r	0.005 p.u
Rotor Inductance	0.156 p.u
Mutual Inductance L_m	2.9 p.u
Pair of poles	3
Back to Back converter Data	
Nominal DC voltage	1200 V
DC capacitance	0.06 F
Wind Turbine data	
Pitch controller gain (K_p)	500
Max. pitch angle	45^0

Table 2 Controller Parameters

λ_1	1.5
λ_2	2.5
λ_3	0.01
λ_4	0.001
l	0.4

A power system is highly nonlinear and stochastic, and is subjected to various kinds of disturbance. This necessitates the use of RED to differentiate noisy relative speed deviations rather than a conventional differentiator. Realistic noise in the PMU measurements is considered in the first case, in which Gaussian noise with zero mean and covariance of 10^{-5} is added to the speed measurements. Figure 13 depicts the significance of RED. As seen, without RED, noise is amplified by the differentiator and this in turn affects the controller performance, while the relative rotor speed and its derivative estimated using RED show significant improvements. Figure 14 depicts the relative rotor angle deviations and it can be concluded that the proposed composite sliding mode shows superior performance even under noisy environment when compared with twisting control.

5 Conclusions

A composite WAC has been proposed to suppress inter-area oscillations by controlling the reactive power output of the DFIG system during disturbances. There are three main contributions of the proposed method. First, a robust differentiator is developed to obtain the real-time differentiation of the relative rotor speed signal of the uncertain nonlinear power system. Second, super twisting control is extended by adding an integral control term to form a robust DI controller to stabilize power oscillations even under non-vanishing disturbances. Control chattering is avoided as the control input is a continuous signal. Third, the robust differentiator is combined with a discontinuous integral controller to build a WAC, which is robust to disturbances affecting the stability of the system.

The proposed control is tested on the benchmark two-area power system model with a DFIG wind energy integration. The results for a three-phase fault in the power system have illustrated that the proposed composite control significantly improves the transient stability of the power system even under non-vanishing disturbances. In the event of three-phase faults, relative rotor angle deviations with DI control can be damped earlier than with conventional methods, while RED is very useful for obtaining the real-time differentiation with reduced noise impact. WAC can be designed in coordination with local PSS to further enhance system transient stability.

6 Nomenclature

DI Discontinuous integral
RED Robust Exact Differentiator
WAC Wide area control
RSC Rotor side converter
GSC Grid side converter
ν Zero mean measurement noise
δ Generator power angle
ω Generator rotor speed
H Generator inertia
P Mechanical input power
P_L Active power demand
V Terminal voltage
Q_w Reactive power supplied by the DFIG system
ΔQ_w Reactive power for damping
Q_{s0} Reactive power supplied by synchronous generators and shunt capacitors$X$ Line reactance
$E'_{d.q}$ Voltage across transient reactance on the d-axis and q-axis
L_m Mutual inductance
T'_0 Time constant of the rotor circuit
u_s Stator terminal voltage
u_r Rotor terminal voltage
R_s Stator resistance
X_s Stator reactance
X'_s Stator transient reactance
i_s Stator current

L_{ss}, L_{rr} Stator and rotor self-inductances
σ Sliding surface
z_1 Estimates of σ
z_2 Estimates of $\dot{\sigma}$
d Cumulative disturbance
λ_1, λ_2,λ_3,λ_4 DI controller parameters
P_{ref} Reference active power
P_g DFIG generated power
Q_{ref} Reference reactive power
K_{p1}, K_{p2}, K_{p3}, K_{i1}, K_{i2}, K_{i3} PI controller parameters
e_p, e_w Active and reactive power errors
e_d, e_q Current errors
u^*_{dr}, u^*_{dr} Control voltages
i_{dr_ref}, i_{qr_ref} Current references

7 Appendix

Details of conventional controller:

The transfer function of the traditional controller is given by (30):

$$H(s) = 10\left(\frac{10s}{1+10s}\right)\left(\frac{1+0.07s}{1+0.21s}\right) \tag{31}$$

Acknowledgements
Not applicable.

Author's contributions
TSLVAR contributed to analysis, modelling, manuscript preparation, revision and typesetting of the manuscript. TSLVAR read and approved the final manuscript.

Funding
The authors declare that the research is not funded by any Government/ Private institution/agency.

Availability of data and materials
All the data is given in the paper or properly cited wherever necessary.

Competing interests
The authors declare that they have no competing interests.

Received: 28 January 2020 Accepted: 22 October 2020
Published online: 22 November 2020

References

1. Punda, L., Capuder, T., Pandžić, H., & Delimar, M. (2017). Integration of renewable energy sources in Southeast Europe: A review of incentive mechanisms and feasibility of investments. *Renewable and Sustainable Energy Reviews*, *71*, 77–88.
2. Lin, W., Wen, J., Cheng, S., & Lee, W.-J. (2012). An investigation on the active-power variations of wind farms. *IEEE Transactions on Industry Applications*, *48*(3), 1087–1094.
3. Luo, J., Zhao, H., Gao, S., & Han, M. (2020). A low voltage ride through strategy of DFIG based on explicit model predictive control. *International Journal of Electrical Power & Energy Systems*, *119*, 105783.
4. Liu, X., Han, Y., & Wang, C. (2017). Second-order sliding mode control for power optimisation of DFIG-based variable speed wind turbine. *IET Renewable Power Generation*, *11*(2), 408–418.
5. Han, Y., & Ma, R. (2019). Adaptive-gain second-order sliding mode direct power control for wind-turbine-driven DFIG under balanced and unbalanced grid voltage. *Energies*, *12*(20), 3886.
6. Tang, Y., Ju, P., Member, S., He, H., Qin, C., & Wu, F. (2013). Optimized control of DFIG-based wind generation using sensitivity analysis and particle swarm optimization. *IEEE Transactions on Smart Grid*, *4*(1), 509–520.
7. Yang, L., Yang, G. Y., Xu, Z., Dong, Z. Y., Wong, K. P., & Ma, X. (2010). Optimal controller design of a doubly-fed induction generator wind turbine system for small signal stability enhancement. *IET Generation Transmission and Distribution*, *4*(5), 579.
8. Wang, L., & Truong, D. N. (2013). Stability enhancement of DFIG-based offshore wind farm fed to a multi-machine system using a STATCOM. *IEEE Transactions on Power Apparatus and Systems*, *28*(3), 2882–2889.
9. Wu, F., Zhang, X.-P., Ping, J., & Sterling, M. J. H. (2008). Decentralized nonlinear control of wind turbine with doubly fed induction generator. *IEEE Transactions on Power Apparatus and Systems*, *23*(2), 613–621.
10. Chang, Y., Hu, J., & Yuan, X. (2020). Mechanism analysis of DFIG-based wind Turbine's fault current during LVRT with equivalent inductances. *IEEE Journal of Emerging and Selected Topics in Power Electronics*, *8*(2), 1515–1527.
11. Shen, Y.-W., Yuan, J.-R., Shen, F.-F., Xu, J.-Z., Li, C.-K., & Wang, D. (2019). Finite control set model predictive control for complex energy system with large-scale wind power. *Complexity*, *2019*, 1–13.
12. Wang, N., Kang, C., & Ren, D. (2015). *Large-Scale Wind Power Grid Integration: Technological and Regulatory Issues*. Elsevier.
13. Messina, A. R., Begovich, O., López, J. H., & Reyes, E. N. (2004). Design of multiple FACTS controllers for damping inter-area oscillations: A decentralised control approach. *International Journal of Electrical Power & Energy Systems*, *26*(1), 19–29.
14. Singh, B., Mukherjee, V., & Tiwari, P. (2015). A survey on impact assessment of DG and FACTS controllers in power systems. *Renewable and Sustainable Energy Reviews*, *42*, 846–882.
15. Messina, A., Begovich, M. O., & Nayebzadeh, M. (1999). Analytical investigation of the use of static VAR compensators to aid damping of inter-area oscillations. *International Journal of Electrical Power & Energy Systems*, *21*(3), 199–210.
16. Hughes, F. M., Anaya-Lara, O., Jenkins, N., & Strbac, G. (2006). A power system stabilizer for DFIG-based wind generation. *IEEE Transactions on Power Apparatus and Systems*, *21*(2), 763–772.
17. Fan, L., Yin, H., & Miao, Z. (2011). On active/reactive power modulation of DFIG-based wind generation for Interarea oscillation damping. *IEEE Transactions on Energy Conversion*, *26*(2), 513–521.
18. Zhang, C., Ke, D., Sun, Y., Chung, C. Y., Xu, J., & Shen, F. (2018). Coordinated supplementary damping control of DFIG and PSS to suppress inter-area oscillations with optimally controlled plant dynamics. *IEEE Transactions on Sustainable Energy*, *9*(2), 780–791.
19. Feng, S., Jiang, P., & Wu, X. (2017). Suppression of power system forced oscillations based on PSS with proportional-resonant controller. *International Transactions on Electrical Energy Systems*, *27*(7), e2328.
20. Singh, M., Allen, A. J., Muljadi, E., Gevorgian, V., Zhang, Y., & Santoso, S. (2015). Interarea oscillation damping controls for wind power plants. *IEEE Transactions on Sustainable Energy*, *6*(3), 967–975.
21. Tsourakis, G., Nomikos, B. M., & Vournas, C. D. (2009). Contribution of doubly fed wind generators to oscillation damping. *IEEE Transactions on Energy Conversion*, *24*(3), 783–791.
22. Surinkaew, T., & Ngamroo, I. (2017). Two-level coordinated controllers for robust inter-area oscillation damping considering impact of local latency. *IET Generation Transmission and Distribution*, *11*(18), 4520–4530.
23. Liao, K., He, Z., Wang, Y., & Yang, J. (2018). An input-output linearization algorithm-based inter-area damping control strategy for DFIG. *IEEJ Transactions on Electrical and Electronic Engineering*, *13*(1), 32–37.
24. Tang, Y., He, H., Wen, J., & Liu, J. (2015). Power system stability control for a wind farm based on adaptive dynamic programming. *IEEE Transactions on Smart Grid*, *6*(1), 166–177.
25. Ma, Y., Liu, J., Liu, H., & Zhao, S. (2018). Active-Reactive Additional Damping Control of a Doubly-Fed Induction Generator Based on Active Disturbance Rejection Control. *Energies*, *11*(5), 1314.
26. Liu, C., Cai, G., Ge, W., Yang, D., Liu, C., & Sun, Z. (2018). Oscillation analysis and wide-area damping control of DFIGs for renewable energy power systems using line modal potential energy. *IEEE Transactions on Power Apparatus and Systems*, *33*(3), 3460–3471.
27. Liao, K., He, Z., Xu, Y., Chen, G., Dong, Z. Y., & Wong, K. P. (2017). A sliding mode based damping control of DFIG for Interarea power oscillations. *IEEE Transactions on Sustainable Energy*, *8*(1), 258–267.
28. Liao, K., Xu, Y., He, Z., & Dong, Z. Y. (2017). Second-order sliding mode based P-Q coordinated modulation of DFIGs against Interarea oscillations. *IEEE Transactions on Power Apparatus and Systems*, *32*(6), 4978–4980.

29. Sanchez, T., Moreno, J. A., & Fridman, L. M. (Oct. 2018). Output feedback continuous twisting algorithm. *Automatica*, *96*, 298–305.
30. Ortiz-Ricardez, F. A., Sanchez, T., & Moreno, J. A. (2015). Smooth Lyapunov function and gain design for a Second Order Differentiator. In *2015 54th IEEE Conference on Decision and Control (CDC)*, (pp. 5402–5407).
31. Moreno, J. A. (2016). Discontinuous integral control for mechanical systems. In *2016 14th International Workshop on Variable Structure Systems (VSS)*, (pp. 142–147).
32. Moreno, J. A. (2018). Discontinuous integral control for systems with relative degree two. In *New perspectives and applications of modern control theory*, (pp. 187–218). Cham: Springer International Publishing.